The spatial distribution of coupling between tau and neurodegeneration in amyloid-β positive mild cognitive impairment

Belfin Robinson[1], Shankar Bhamidi[2], and Eran Dayan[1,3], for the Alzheimer's Disease Neuroimaging Initiative

[1]Biomedical Research Imaging Center, University of North Carolina at Chapel Hill, Chapel Hill, North Carolina, USA.
[2]Department of Statistics and Operations Research, University of North Carolina at Chapel Hill, Chapel Hill, North Carolina, USA
[3]Department of Radiology, University of North Carolina at Chapel Hill, Chapel Hill, North Carolina, USA.

Corresponding author
Eran Dayan,
Associate Professor of Radiology,
University of North Carolina at Chapel Hill.
Email: eran_dayan@med.unc.edu

Short/running title.
Coupling between tau and neurodegeneration in MCI

Keywords: Mild cognitive impairment, amyloid-β, Tau, Atrophy, Multilayer network, neurodegeneration

ABSTRACT

Background:
Synergies between amyloid-β (Aβ), tau, and neurodegeneration persist along the Alzheimer's disease (AD) continuum. This study aimed to evaluate the extent of spatial coupling between tau and neurodegeneration (atrophy) and its relation to Aβ positivity in mild cognitive impairment (MCI).

Methods:
Data from 409 subjects were included (95 cognitively normal controls, 158 Aβ positive (Aβ+) MCI, and 156 Aβ negative (Aβ-) MCI) Florbetapir PET, Flortaucipir PET, and structural MRI were used as biomarkers for Aβ, tau and atrophy, respectively. Individual correlation matrices for tau load and atrophy were used to layer a multilayer network, with separate layers for tau and atrophy. A measure of coupling between corresponding regions of interest/nodes in the tau and atrophy layers was computed, as a function of Aβ positivity. The extent to which tau-atrophy coupling mediated associations between Aβ burden and cognitive decline was also evaluated.

Results:
Heightened coupling between tau and atrophy in Aβ+ MCI was found primarily in the entorhinal and hippocampal regions (i.e., in regions corresponding to Braak stages I/II), and to a lesser extent in limbic and neocortical regions (i.e., corresponding to later Braak stages). Coupling strengths in the right middle temporal and inferior temporal gyri mediated the association between Aβ burden and cognition in this sample.

Conclusions:
Higher coupling between tau and atrophy in Aβ+ MCI is primarily evident in regions corresponding to early Braak stages and relates to overall cognitive decline. Coupling in neocortical regions is more restricted in MCI.

Keywords: Mild cognitive impairment, amyloid-β, Tau, Atrophy, Multilayer network, neurodegeneration

INTRODUCTION

Alzheimer's disease (AD), the most common form of neurodegeneration, has become a key contemporary public health concern (1). While the cause of this disease is still unknown, it is believed to develop from the accumulation of the extracellular amyloid-β (Aβ) peptide and from tangles of hyperphosphorylated tau, which lead to synaptic impairment, neuronal loss (atrophy), and consequently to cognitive and behavioral decline (2). The leading model as to how these pathological processes bind together is known as the amyloid cascade hypothesis (3). According to this influential framework, Aβ pathology initiates alterations in tau which then lead to neurodegeneration and to the cognitive and behavioral manifestations of AD (4).

The serial and linear structure of the amyloid cascade hypothesis has, nevertheless, been challenged in the literature. In particular, studies suggest that Aβ, tau, and neurodegeneration (atrophy) could have synergistic effects in AD pathogenesis (5). Yet, the extent of spatial

coupling between alterations in AD pathological biomarkers, specifically in biomarkers for tau and atrophy remains uncertain(6–9). On the one hand, studies have reported large degrees of spatial overlap throughout the brain between tau burden, as assessed using positron emission tomography (PET), and magnetic resonance imaging (MRI)-based measures of atrophy in both cognitively normal controls and individuals with AD (6). On the other hand, studies have found more restricted spatial coupling between tau and atrophy, which may emerge from heterogeneity in patterns of tau spread (10). Moreover, the majority of studies that examined interactions between tau and atrophy were either in normal controls or in individuals with AD (11,12). The extent of coupling between these biomarkers in individuals with MCI and AD pathologic changes, who can be considered as being at the prodromal stages of AD(13), remains less understood.

Over the last decade, there has been significant interest and methodology development in the study of network valued data over the same node set (e.g., regions in the brain), but across multiple layers (14,15). These method may help in clarifying the extent of coupling that exists between tau and atrophy is via multilayer networks. Multilayer networks allow to model and study complex heterogeneous relationships between entities within a system and variation of these relationships across layers (14,16). In the context of brain networks, multilayer network models were used for understanding the relationships between brain structure, function, and dynamics across multiple scales, both in healthy brain and in AD (15,17,18). We reasoned that the extent of spatial coupling between tau and atrophy could be modeled using multilayer networks, since this approach can allow to inspect interactions both within and between network layers.

In the current study, we used a cross-sectional sample of participants with MCI (n=314), as well as data from cognitively normal (CN) participants (n=95) to reconstruct single-subject multilayer networks that represent tau and atrophy as separate layers, and the interactions among these two biomarkers in-between layers. More specifically, tau PET and structural MRI (atrophy) data from 68 regions of interest (ROIs) were first extracted from MCI and CN participants **(Figure 1A)**. Tau and atrophy data were then z-scored relative to the means and standard deviations from the entire pool of CN participants **(Figure 1B)**. Subsequently, individual-subject covariance matrices were computed for each participant **(Figure 1C)** and used to reconstruct tau and atrophy networks for each participant after minimally thresholding the edge weights to retain all positive weights in the networks **(Figure 1D)**. The tau and atrophy networks were then modeled as multilayer networks and grouped according to Aβ positivity **(Figure 1E)**. This allowed us to study the interaction between the tau and atrophy layers **(Figure 1F)** at the presence and absence of Aβ positivity. We further examined whether the extent of coupling between tau and atrophy differed among transentorhinal, limbic and isocortical ROIs, defined based on the Braak staging system (19). These steps allowed us to evaluate our method for assessment of coupling against an established staging scheme for tau pathology.

METHODS AND MATERIALS

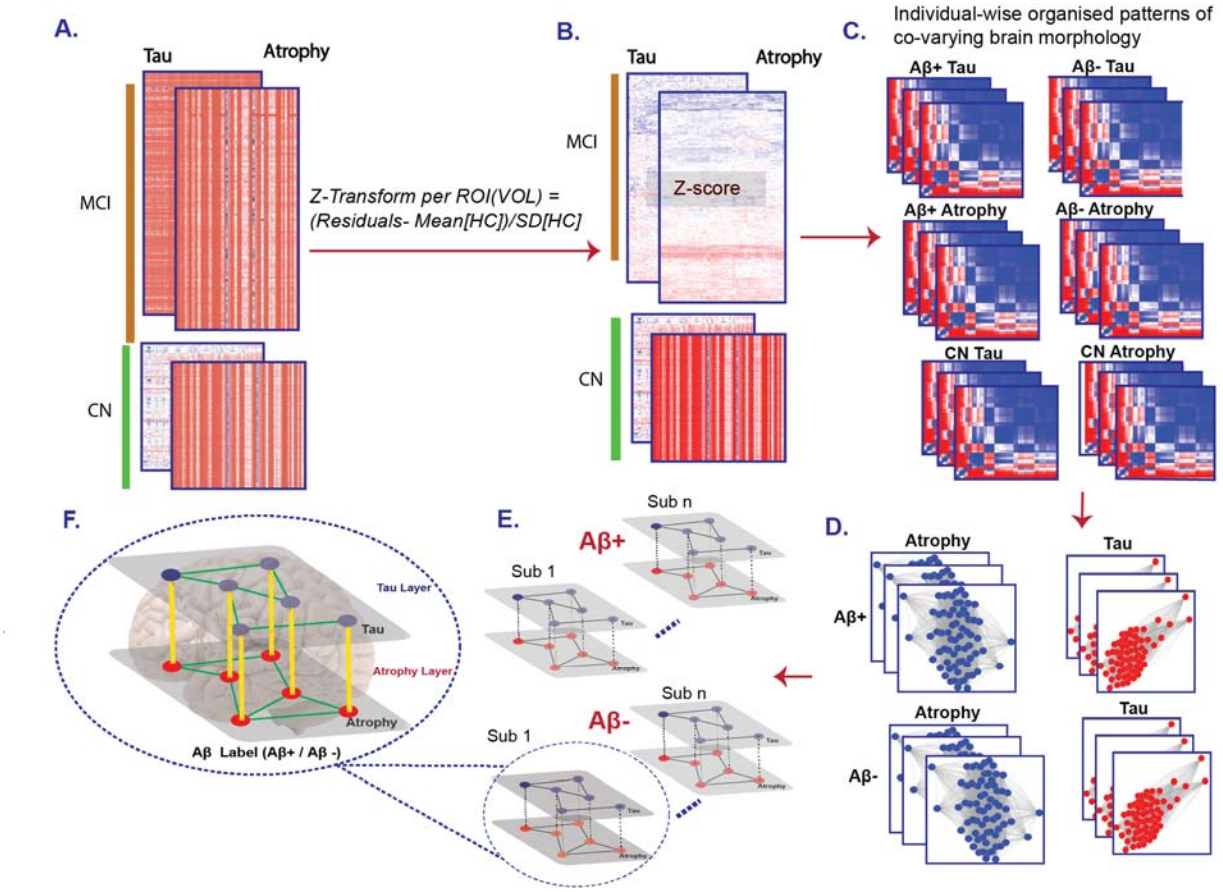

Figure 1: Modeling framework. (A.) Participant' (MCI, CN) tau standardized uptake value ratios (SUVRs) were calculated in 68 regions of interest (ROIs) (B.) Volumetric measures from the same 68 ROIs were used as measures of atrophy. Data was Z-score transformed using means and standard-deviations (SD) from controls (Value – Mean [CN]/ SD[CN]) (C.) Individual-subject structural covariance matrices were reconstructed for tau and atrophy (D.) Covariance matrices for tau and atrophy were then modeled as single layer networks for each individual participant. (E.) Multilayer networks with tau and atrophy serving as single layers were reconstructed and labeled according to Aβ positivity. (F.) Inter-layer (yellow), Intra-layer (green) and cross-layer (grey-dotted) edges in a multilayer network. MCI – Mild Cognitive Impairment, CN – cognitively normal controls.

Participants

Data used in this study were obtained from the Alzheimer's Disease Neuroimaging Initiative (ADNI) dataset (https://ida.loni.usc.edu), including the ADNI-1, ADNI-GO, and ADNI-2 cohorts. A total of 314 MCI participants who had ^{18}F-florbetapir and ^{18}F-flortaucipir PET data were included in the study **(Table 1)**. Additional data from 95 CN participants was additionally used to aid in the reconstruction of individual-subject graphs/networks for each of the MCI participants. ADNI's native inclusion and exclusion criteria were used in both the CN and MCI groups. Participants with MCI were further divided into Aβ positive (Aβ+) and negative (Aβ-), based on an established cutoff **(SUVR > 1.11)**, computed relative to the whole cerebellum reference region (20,21).

Imaging data analysis

Regional florbetapir PET summary data were obtained from ADNI as derived variables (22,23). In short, T1 weighted native-space images were processed with FreeSurfer v7.1.1, and a cortical summary region was defined for each subject, based on frontal, anterior and posterior cingulate, lateral parietal, and lateral temporal ROIs. The T1 images were coregistred to florbetapir PET scans, which allowed to extract PET data from cortical ROI. Standardized uptake value ratio (SUVR's) were then calculated for the cortical summary region, based on the whole cerebellum reference region. SUVR values from the cortical summary region were then used to define Aβ burden and positivity. Regional summary data based on flortaucipir PET were also obtained from ADNI as derived variables. In short, MPRAGE images were parcellated into a set of 68 ROIs **(See Supplementary Figure 1A, Supplementary Figure 1B)** using FreeSurfer v7.1.1 based on the Desikan-Killiany protocol (24). Flortaucipir images were co-registered to the corresponding MPRAGE images to determine the mean regional flortaucipir uptake within each ROI. SUVRs for each of 68 ROIs were then calculated, by dividing uptake values by a cerebellar reference region. Finally, grey matter volumes extracted from the same 68 ROIs using FreeSurfer v7.1.1 were used as measures of regional atrophy.

Network reconstruction

Regional tau uptake and grey matter volume data from MCI subjects were considered for analysis (**Figure 1A**). Data from CN subjects were further used to aid in the reconstruction of single-subject networks/graphs for each subject with MCI (**Figure 1A**). In this procedure, individual covariance networks in the target group, are reconstructed based on their deviation from an averaged network based on a group of controls (25). First, an averaged covariance network was reconstructed from a group of CN subjects (n=95), separately for tau and atrophy. Atrophy and tau data from each MCI subject were then normalized via a z-score transform using the mean and standard deviation of the averaged, CN-based, tau and atrophy networks (**Figure 1B**). This allowed for the reconstruction of single covariance matrices (25,26) for each MCI subject (**Figure 1C**). The covariance matrix is a nROI × nROI matrix, where for each index [x,y] we compare the z-scores of the corresponding tau and atrophy ROIs. The equation is given below:

$$Brain\ structural\ covariance[x,y] = \frac{1}{e^{[(zscore\ of\ x^{th}\ ROI - zscore\ of\ y^{th}\ ROI)^2]}} \qquad (1)$$

Higher values in ROIs within these matrices denote high covariance compared to the corresponding ROIs from the averaged CN-based networks. The matrices generated for tau and atrophy were structured as single-layer networks/graphs **(Figure 1D).** The single-layer graphs were then layered into a two-layered graph with tau and atrophy as separate layers **(Figure 1E).** This form of representation allowed us to examine and compare both intra-layer (green colored edges in **Figure 1F**), and inter-layer edges (yellow-colored edges in **Figure 1F**). While the former type of edges corresponds to covariance for ROIs in the tau and atrophy networks separately, the latter type of edges, which connect the nodes across layers, allow to examine interactions between tau and atrophy. Moreover, unlike multiplex networks, where inter-layer

edges connect the same nodes across layers, the multilayer network representation used here also incorporates inter-layer edges connecting across nodes (grey dotted edges in **Figure 1F**). The multilayer networks were generated using R (Version 4.2.1) (27), with the igraph (Version: 1.3.5) and muxviz (Version: 3.1) (28) libraries.

Interlayer coupling score.

A key objective in the current study was to assess the extent of regional/spatial coupling between tau and atrophy in the presence and absence of Aβ positivity. To that effect we have computed a coupling score between the tau and atrophy layers, based on the distance between the layers (29). As a measure of distance, we used Euclidean distance, as it was previously used to assess coupling between network node sets (30). First, the partitioned distance between the tau and atrophy layers was calculated. The resulting distance matrix D was used to calculate the coupling score. The distance between identical ROIs across layers was defined as (D_r), whereas interlayer edges, connecting different ROIs across the layers were defined as (D_b). The coupling score was computed to measure the relative coupling between tau and atrophy, as the ratio between a spatially coupled edge and all other non-coupled edges:

$$\text{Coupling score} = \frac{D_r - mean(D_b)}{D_r} \quad (2)$$

Partitioned Euclidian distance was computed using the pdist (Version 1.2.1) library (https://github.com/jeffwong/pdist) in R (Version 4.2.1). A toy example of the procedure for calculating coupling scores is illustrated in **supplementary Figure 2**.

Braak Staging

To facilitate the interpretability of the reported results and link them with existing knowledge on the spread of pathology along the AD continuum, we compared atrophy and tau load, as well as coupling between the two, across ROIs known to be affected at different stages along Braak's staging scheme (19,31,32) **(Supplementary Figure 1B).** The analysis compared tau load, atrophy, and coupling between the two in ROIs grouped across the transentorhinal (stages I and II), limbic (stages III and IV), and isocortical (stages V and VI) stages (33).

Statistical Analysis

Group differences in demographic data (age, gender, education) were analyzed using t-tests or chi-squared tests. These analyses were conducted in R, with the packages dgof (v1.4) (https://CRAN.R-project.org/package=dgof). Group differences in tau load and in atrophy, as well as in regional coupling between tau and atrophy were based on a non-parametric, permutation-based analysis of variance, adjusted for age (see **Table 1**). The resulting p-values were False Discovery Rate (FDR) corrected across ROIs. These tests were carried out using the aovperm function, which is part of the permuco (v1.1.1) library (https://github.com/jaromilfrossard/permuco) in R. Finally, we examined whether the association between Aβ burden and cognition, assessed with clinical dementia rating sum of boxes (CDR-SB) scores (34), was mediated by the extent of coupling between tau and atrophy. Parallel mediation analyses were conducted in Python 3, using the pingouin package (Version 0.5.3)

(https://pingouin-stats.org/). Confidence intervals in the mediation model were computed using bootstrapping (10,000 steps).

RESULTS

Group demographics

Our objective was to compare the extent of coupling between tau and atrophy in the presence and absence of Aβ positivity. To that effect, we divided a total of 314 individuals with MCI into two groups, Aβ + (n=158) and Aβ - (n=156), based on Aβ PET data and established cutoffs ((20,21), see Methods). The Aβ + and Aβ - groups did not show significant differences in sex (p=0.364) or education (p=0.536) but did differ in age (p= 0.0288) **(Table 1)**.

Table 1 Characteristics of data used in the study.

Measure	**Aβ +**	**Aβ -**
Age (years) *	71.13 ± 6.96	70.28 ± 6.71
Sex	Female: 81 (51) Male: 77 (49)	Female:72 (46) Male: 84 (54)
Education (years)	16.34 ± 2.60	16.52 ± 2.65

Values are given as mean ± standard deviation or percentages (%); * denotes significant group difference (p<0.05); Aβ- amyloid-β

Tau load and atrophy levels in Aβ + and Aβ - subjects

We first examined group difference between Aβ + and Aβ - subjects in tau load and in atrophy, grouping ROIs across the transentorhinal (stages I and II), limbic (stages III and IV), and isocortical (stages V and VI) Braak stages (33) **(Figure 2A)**. Age corrected mean levels of tau load **(Figure 2B)** were significantly different between the two groups in ROIs implicated in Braak stages I/II ($p<0.001$), III/IV ($p<0.001$), and V/VI ($p<0.001$). Similarly, age corrected mean levels of atrophy **(Figure 2C)** showed significant differences between the two groups in ROIs corresponding to Braak stages I/II ($p<0.001$), III/IV ($p=0.0026$), and V/VI ($p=0.0332$). In both comparisons, significant differences were retained when outlier values were removed.

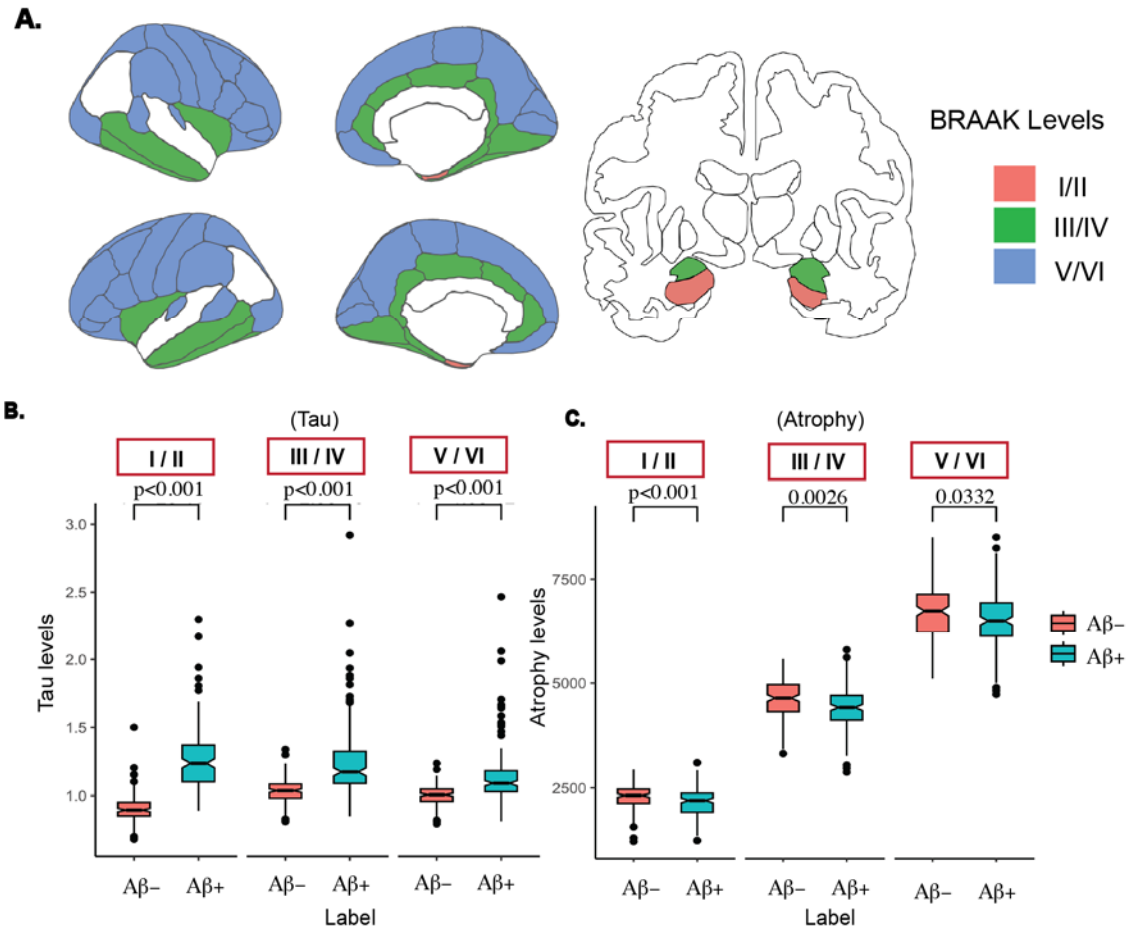

Figure 2: Group comparisons for tau load and atrophy (A.) Analysis was performed separately for regions of interest (ROIs) grouped according to the transentorhinal (stages I/II), limbic (stages III/IV) and isocortical (stages V/VI) Braak stages. (B.) The Aβ+ group showed greater tau uptake than the Aβ- group in ROIs corresponding to Braak I/II, Braak III/ IV and Braak V/VI. (C) The Aβ+ group also showed higher atrophy levels when compared to the Aβ- group in the same grouped ROIs.

Coupling between tau and atrophy

We next examined the regional coupling between tau and atrophy, and the extent to which it differed as a function of Aβ positivity. Taking advantage of the multilayer representation of tau and atrophy as separate layers composed of identical nodes (ROIs), we computed a coupling score between tau and atrophy, based on the Euclidean distance between the layers **(Figure 3A).** The coupling score denoted the ratio between each spatially coupled edge and all other non-coupled edges in the multilayer network (**Figure 3B**; see Methods). In all regions corresponding to Braak I/II **(Figure 3B)**, the Aβ+ group showed significantly greater coupling (FDR corrected) in the left ($p = 0.0008$) and right entorhinal ($p = 0.0008$), as well as left ($p = 0.03946$) and right hippocampal ($p = 0.048$) ROIs. For ROIs corresponding to Braak III/IV **(Figure 3C)** the Aβ+ group showed significantly greater (FDR corrected) coupling in left lingual ($p=0.020$), right fusiform ($p=0.004$), right middle temporal ($p=0.020$), right insula ($p=0.02$) and right inferior temporal ($p=0.02$) ROIs. Altogether 20.8% of the regions in Braak III/IV showed significant coupling between tau and atrophy. Finally, for ROIs corresponding to Braak V/VI **(Figure 3D)** the Aβ+ group showed greater coupling (FDR corrected) in the left traverse temporal

(p=0.0173), right superior frontal (p=0.0173), right lateral orbitofrontal (p=0.008), right superior parietal (p=0.044), right precuneus (p=0.019), right traverse temporal (p=0.004), right postcentral (p=0.012), right precentral (p=0.031), and right paracentral (p=0.004) ROIs. Overall, 22.5% of the ROIs in Braak V/VI showed significant coupling between tau and atrophy.

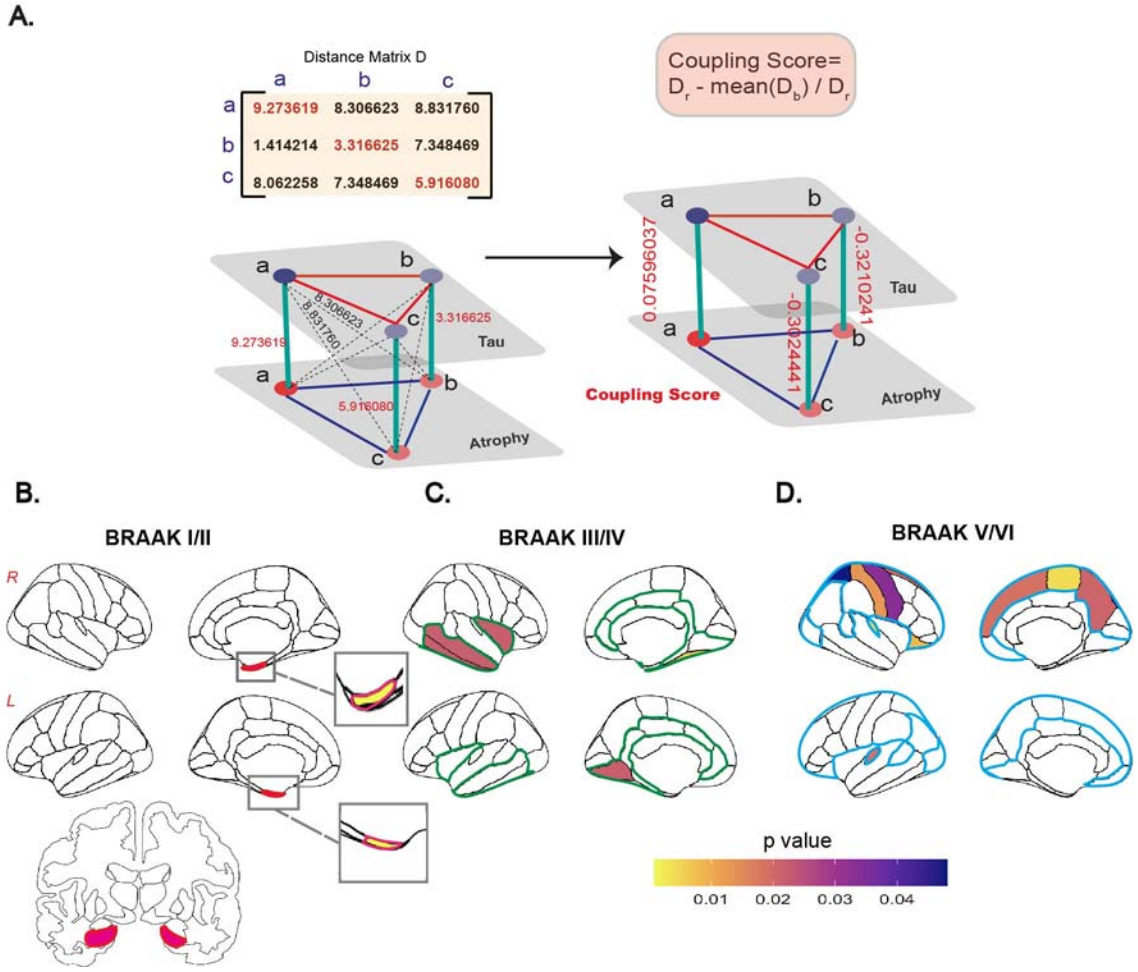

Figure 3: Coupling between tau and atrophy. (A.) Calculation of coupling scores computed to measure the relative coupling between tau and atrophy, was based on the Euclidean distance between layers (distance matrix D) and denotes the ratio between a spatially coupled edge D_r (red) and all other non-coupled edges D_b (black). (B.) ROIs implicated in Braak I/II stages that showed significantly higher coupling in the Aβ+ group, as compared to the Aβ- group (C.) ROIs corresponding to Braak III/IV where significantly higher coupling was found in the Aβ+ group, compared to the Aβ- group (D.) ROIs implicated in Braak V/VI that showed significantly higher coupling in the Aβ+ group, compared to the Aβ- group. Contours depict the entire set of ROIs implicated in each of the stages (corresponding to Figure 2A).

Mediational link between Aβ burden cognition and tau-atrophy coupling

Our results so far reveal differential levels of coupling between tau and atrophy when comparing Aβ+ and Aβ- subjects. Next, we examined whether the extent of coupling and its relationship with Aβ burden also relates to subjects' cognitive status. Considering Aβ as a continuous

variable, we next tested whether the association between Aβ burden and global cognition, assessed with CDR-SB scores, were mediated by the extent of coupling between tau and atrophy (considering ROIs where coupling scores were found to be significant). This was achieved by fitting the data with a parallel mediation model. We found that coupling in the right middle temporal (p = 0.005) and right inferior temporal (p = 0.0288) ROIs (typically implicated in Braak III/IV) significantly mediated the association between of Aβ burden and CDR-SB scores **(Figure 4).**

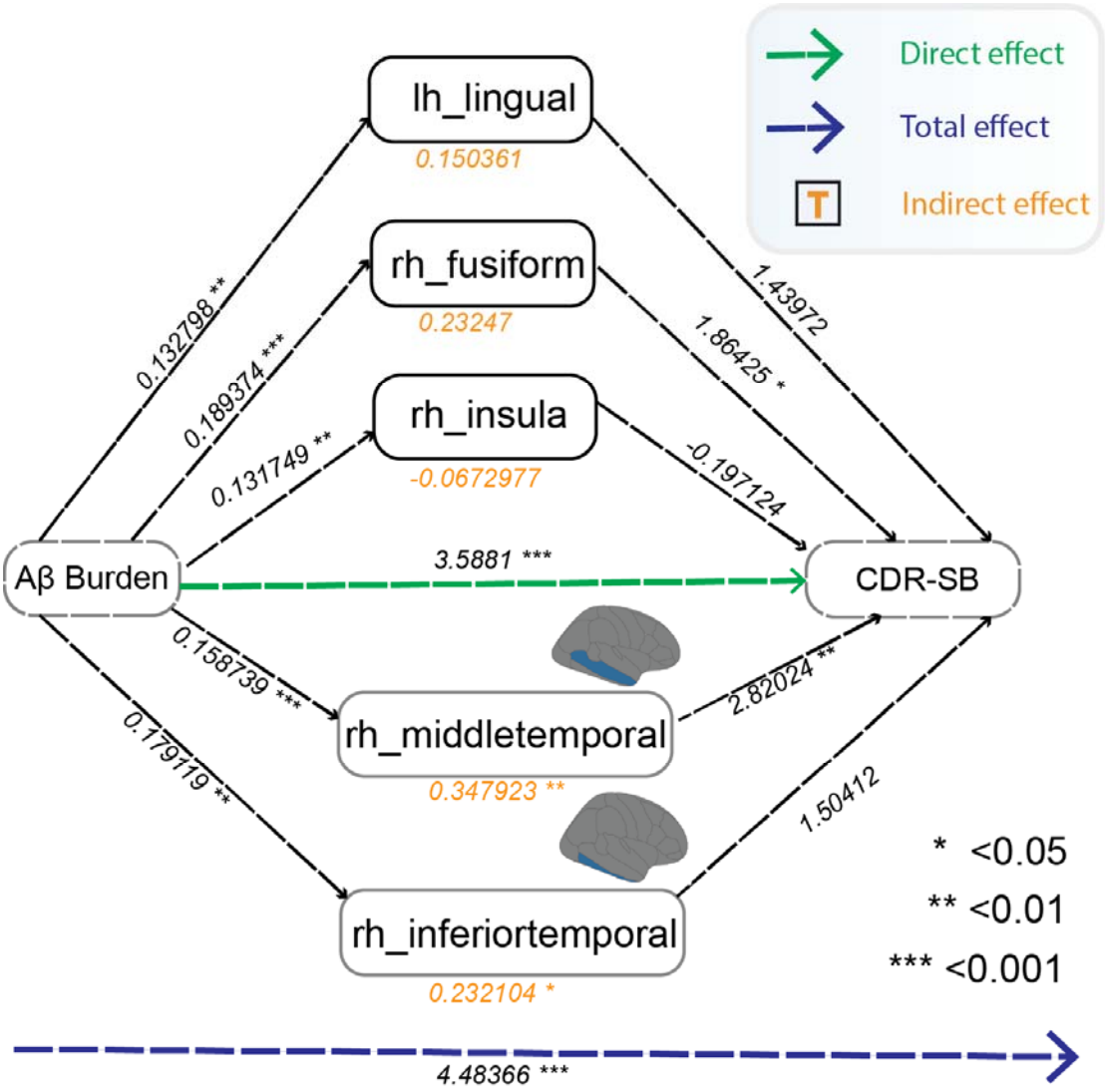

Figure 4: Mediational link between Aβ burden, coupling between tau and atrophy and global cognition. The association between Aβ burden, considered as a continuous variable, and global cognition (CDR-SB: Clinical Dementia Rating Scale–Sum of Boxes) was mediated by coupling between tau and atrophy in the right middle temporal (p=0.005) and right inferior temporal (p=0.02) cortices. Direct, indirect (mediation) and direct effects are shown.

DISCUSSION

The objective of the current study was to estimate the extent of spatial coupling between tau and atrophy biomarkers in individuals with MCI, study the role of Aβ burden in this coupling, and examine the relationship between coupling and cognitive dysfunction. Overall, stronger coupling between tau and atrophy was observed in Aβ+ as compared to Aβ - individuals with MCI. The extent of coupling differences between these two groups varied spatially. Whereas strong coupling was observed in all ROIs corresponding to the transentorhinal stages (Braak stages I/II), more restricted coupling was found in ROIs from the limbic (stages III/IV) and isocortical (stages V/VI) stages. Finally, our results reveal that coupling between tau and atrophy in the middle temporal and inferior temporal cortices mediated the association between Aβ burden and cognitive dysfunction.

Stronger coupling between tau and atrophy was found in the Aβ+ group, relative to the Aβ - group in all ROIs corresponding to the early transentorhinal stages (Braak stages I/II), including the entorhinal cortex and the hippocampus. Early involvement of these regions in AD pathogenesis is well documented (35–37). Moreover, atrophy in the hippocampus and adjacent early Braak regions is predictive of conversion from MCI to AD (38,39). Association between tau and atrophy in regions corresponding to early Braak stages are also evident in Aβ- CN individuals (40), however the current results demonstrate that coupling was stronger when Aβ load was greater. Furthermore, the strong local coupling observed here in early Braak regions is consistent with the observation that in MCI and AD, stronger local, but not distant coupling exists between tau PET load and cortical atrophy in these regions (41).

In regions considered as being part of the limbic (stages III/IV) and isocortical (stages V/VI) Braak stages, coupling between tau and atrophy was more restricted. Altogether, approximately 20% of the ROIs affected at these mid and later Braak stages showed stronger tau-atrophy coupling in the Aβ+, relative to the Aβ - group. Of note, group differences in atrophy in ROIs corresponding to stages V/VI were rather small, thus any findings on coupling seen among these ROIs should be interpreted with caution. The more restricted level of local coupling between tau and atrophy in ROIs corresponding to later Braak stages is consistent with earlier results (41). Considering that individuals with MCI, who are along the AD continuum, are likely at stages III/IV (42), lower levels of coupling in ROIs corresponding to higher Braak stages is expected. Additional research is needed to further delineate the correspondence between neuropathological burden and coupling observed between *in-vivo* imaging biomarkers.

We report that the association between Aβ burden and global cognition, as captured by CDR-SB scores is mediated by the extent of tau-atrophy coupling in right middle temporal and right inferior temporal cortices. Early involvement of these cortical regions in AD pathology has been reported (43). Moreover, middle, and inferior temporal regions, and ROIs belonging to Braak stage III in general, were noted as critical regions in rapid conversion from MCI to AD (44,45). Altogether, our findings join these earlier observations in highlighting the contribution of pathology in the temporal lobe to cognitive dysfunction at the prodromal phases on AD.

In the current study we queried the extent of coupling between tau and atrophy by modeling multimodal neuroimaging data as a multilayer network. Multilayer networks can aid in modeling complex interactions that occur among biological (or non-biological) processes that operate at differing spatial and temporal scales (46). This approach may thus properly capture the heterogeneity often observed in biological systems which may result from the diverse interactions of the system's various substrates (47). Here, the multilayer representation allowed us to compare coupled versus non-coupled interactions among 2 distinct biological processes characteristic of the AD continuum. Future work can focus on other processes and mechanisms which can be quantified in multilayer networks, such as changes in modularity (48,49) redundancy (50), and robustness (51,52), known to be strongly impacted by aging and dementia (53–57).

Summary

In summary, we report that coupling between tau and atrophy existed throughout the brain but was more prominent in regions that are known to be affected at the transentorhinal stages of AD pathology. Altogether, these results highlight the centrality of coupling between tau and atrophy at the prodromal phases of AD.

ACKNOWLEDGMENTS AND DISCLOSURES

We thank William for valuable feedback. Research reported in this publication was supported by the National Institute on Aging of the National Institutes of Health under Award Number R01AG062590. We would also like to acknowledge NSF DMS-2113662 and NSF RTG grant DMS-2134107 for their support. The content is solely the responsibility of the authors and does not necessarily represent the official views of the National Institutes of Health. Data used in preparation of this article were obtained from the Alzheimer's Disease Neuroimaging Initiative (ADNI) database (adni.loni.usc.edu). As such, the investigators within the ADNI contributed to the design and implementation of ADNI and/or provided data but did not participate in analysis or writing of this report. A complete listing of ADNI investigators can be found at: http://adni.loni.usc.edu/wp-content/uploads/how_to_apply/ADNI_Acknowledgement_List.pdf

Disclosures

The authors have no conflicts of interest or any financial interests to disclose.

References

1. Nichols E, Szoeke CEI, Vollset SE, Abbasi N, Abd-Allah F, Abdela J, *et al.* (2019): Global, regional, and national burden of Alzheimer's disease and other dementias, 1990–2016: a systematic analysis for the Global Burden of Disease Study 2016. *Lancet Neurol* 18. https://doi.org/10.1016/S1474-4422(18)30403-4
2. Kumar A, Singh A, Ekavali (2015): A review on Alzheimer's disease pathophysiology and its management: An update. *Pharmacological Reports*, vol. 67. https://doi.org/10.1016/j.pharep.2014.09.004
3. Ricciarelli R, Fedele E (2017): The Amyloid Cascade Hypothesis in Alzheimer's Disease: It's Time to Change Our Mind. *Curr Neuropharmacol* 15. https://doi.org/10.2174/1570159x15666170116143743
4. Karran E, Mercken M, Strooper B De (2011): The amyloid cascade hypothesis for Alzheimer's disease: An appraisal for the development of therapeutics. *Nature Reviews Drug Discovery*, vol. 10. https://doi.org/10.1038/nrd3505
5. Busche MA, Hyman BT (2020): Synergy between amyloid-β and tau in Alzheimer's disease. *Nature Neuroscience*, vol. 23. pp 1183–1193.
6. Xia C, Makaretz SJ, Caso C, McGinnis S, Gomperts SN, Sepulcre J, *et al.* (2017): Association of in vivo [18F]AV-1451 tau PET imaging results with cortical atrophy and symptoms in typical and atypical Alzheimer disease. *JAMA Neurol* 74. https://doi.org/10.1001/jamaneurol.2016.5755
7. Sepulcre J, Schultz AP, Sabuncu M, Gomez-Isla T, Chhatwal J, Becker A, *et al.* (2016): In vivo tau, amyloid, and gray matter profiles in the aging brain. *Journal of Neuroscience* 36. https://doi.org/10.1523/JNEUROSCI.0639-16.2016
8. LaPoint MR, Chhatwal JP, Sepulcre J, Johnson KA, Sperling RA, Schultz AP (2017): The association between tau PET and retrospective cortical thinning in clinically normal elderly. *Neuroimage* 157. https://doi.org/10.1016/j.neuroimage.2017.05.049
9. Mak E, Bethlehem RAI, Romero-Garcia R, Cervenka S, Rittman T, Gabel S, *et al.* (2018): In vivo coupling of tau pathology and cortical thinning in Alzheimer's disease. *Alzheimer's and Dementia: Diagnosis, Assessment and Disease Monitoring* 10. https://doi.org/10.1016/j.dadm.2018.08.005
10. Mohanty R, Ferreira D, Nordberg A, Westman E (2023): Associations between different tau-PET patterns and longitudinal atrophy in the Alzheimer's disease continuum: biological and methodological perspectives from disease heterogeneity. *Alzheimers Res Ther* 15. https://doi.org/10.1186/s13195-023-01173-1
11. Liu G, Liu C, Qiu A (2021): Spatial correlation maps of the hippocampus with cerebrospinal fluid biomarkers and cognition in Alzheimer's disease: A longitudinal study. *Hum Brain Mapp* 42. https://doi.org/10.1002/hbm.25414
12. Digma LA, Madsen JR, Reas ET, Dale AM, Brewer JB, Banks SJ (2019): Tau and atrophy: Domain-specific relationships with cognition. *Alzheimers Res Ther* 11. https://doi.org/10.1186/s13195-019-0518-8
13. Jack CR, Bennett DA, Blennow K, Carrillo MC, Dunn B, Haeberlein SB, *et al.* (2018): NIA-AA Research Framework: Toward a biological definition of Alzheimer's disease. *Alzheimer's & Dementia* 14: 535–562.

14. Kivelä M, Arenas A, Barthelemy M, Gleeson JP, Moreno Y, Porter MA, *et al.* (2014): Multilayer networks. *J Complex Netw* 2: 203–271.
15. De Domenico M (2017): Multilayer modeling and analysis of human brain networks. *GigaScience*, vol. 6. https://doi.org/10.1093/gigascience/gix004
16. Boccaletti S, Bianconi G, Criado R, del Genio CI, Gómez-Gardeñes J, Romance M, *et al.* (2014): The structure and dynamics of multilayer networks. *Phys Rep* 544: 1–122.
17. Guillon J, Chavez M, Battiston F, Attal Y, La Corte V, de Schotten MT, *et al.* (2019): Disrupted core-periphery structure of multimodal brain networks in Alzheimer's disease. *Network Neuroscience* 3. https://doi.org/10.1162/netn_a_00087
18. Cai L, Wei X, Liu J, Zhu L, Wang J, Deng B, *et al.* (2020): Functional Integration and Segregation in Multiplex Brain Networks for Alzheimer's Disease. *Front Neurosci* 14. https://doi.org/10.3389/fnins.2020.00051
19. Braak H, Thal DR, Ghebremedhin E, Del Tredici K (2011): Stages of the pathologic process in alzheimer disease: Age categories from 1 to 100 years. *J Neuropathol Exp Neurol* 70. https://doi.org/10.1097/NEN.0b013e318232a379
20. Landau SM, Mintun MA, Joshi AD, Koeppe RA, Petersen RC, Aisen PS, *et al.* (2012): Amyloid deposition, hypometabolism, and longitudinal cognitive decline. *Ann Neurol* 72. https://doi.org/10.1002/ana.23650
21. S.M. L, M. L, A.D. J, M. P, M.A. M, J.Q. T, *et al.* (2013): Comparing positron emission tomography imaging and cerebrospinal fluid measurements of (beta)-amyloid. *Ann Neurol* 74.
22. Landau SM, Marks SM, Mormino EC, Rabinovici GD, Oh H, O'Neil JP, *et al.* (2012): Association of lifetime cognitive engagement and low β-amyloid deposition. *Arch Neurol* 69. https://doi.org/10.1001/archneurol.2011.2748
23. Landau SM, Breault C, Joshi AD, Pontecorvo M, Mathis CA, Jagust WJ, Mintun MA (2013): Amyloid-β imaging with Pittsburgh compound B and florbetapir: Comparing radiotracers and quantification methods. *Journal of Nuclear Medicine* 54. https://doi.org/10.2967/jnumed.112.109009
24. Desikan RS, Ségonne F, Fischl B, Quinn BT, Dickerson BC, Blacker D, *et al.* (2006): An automated labeling system for subdividing the human cerebral cortex on MRI scans into gyral based regions of interest. *Neuroimage* 31. https://doi.org/10.1016/j.neuroimage.2006.01.021
25. Yun JY, Boedhoe PSW, Vriend C, Jahanshad N, Abe Y, Ameis SH, *et al.* (2020): Brain structural covariance networks in obsessive-compulsive disorder: A graph analysis from the ENIGMA consortium. *Brain* 143: 684–700.
26. Yun JY, Jang JH, Kim SN, Jung WH, Kwon JS (2015): Neural Correlates of Response to Pharmacotherapy in Obsessive-Compulsive Disorder: Individualized Cortical Morphology-Based Structural Covariance. *Prog Neuropsychopharmacol Biol Psychiatry* 63. https://doi.org/10.1016/j.pnpbp.2015.06.009
27. Team RC (2021): R: A Language and Environment for Statistical Computing. *R Foundation for Statistical Computing*.
28. de Domenico M, Porter MA, Arenas A (2015): MuxViz: A tool for multilayer analysis and visualization of networks. *J Complex Netw* 3. https://doi.org/10.1093/comnet/cnu038
29. Shimada Y, Hirata Y, Ikeguchi T, Aihara K (2016): Graph distance for complex networks. *Sci Rep* 6. https://doi.org/10.1038/srep34944

30. Liu ZQ, Vázquez-Rodríguez B, Spreng RN, Bernhardt BC, Betzel RF, Misic B (2022): Time-resolved structure-function coupling in brain networks. *Commun Biol* 5. https://doi.org/10.1038/s42003-022-03466-x
31. Braak H, Braak E (1995): Staging of alzheimer's disease-related neurofibrillary changes. *Neurobiol Aging* 16. https://doi.org/10.1016/0197-4580(95)00021-6
32. Braak H, Alafuzoff I, Arzberger T, Kretzschmar H, Tredici K (2006): Staging of Alzheimer disease-associated neurofibrillary pathology using paraffin sections and immunocytochemistry. *Acta Neuropathol* 112. https://doi.org/10.1007/s00401-006-0127-z
33. Braak H, Braak E (1991): Neuropathological stageing of Alzheimer-related changes. *Acta Neuropathologica*, vol. 82. https://doi.org/10.1007/BF00308809
34. O'Bryant SE (2008): Staging Dementia Using Clinical Dementia Rating Scale Sum of Boxes Scores. *Arch Neurol* 65. https://doi.org/10.1001/archneur.65.8.1091
35. Duyckaerts C, Braak H, Brion JP, Buée L, del Tredici K, Goedert M, *et al.* (2015): PART is part of Alzheimer disease. *Acta Neuropathol* 129. https://doi.org/10.1007/s00401-015-1390-7
36. Stoub TR, Rogalski EJ, Leurgans S, Bennett DA, deToledo-Morrell L (2010): Rate of entorhinal and hippocampal atrophy in incipient and mild AD: Relation to memory function. *Neurobiol Aging* 31. https://doi.org/10.1016/j.neurobiolaging.2008.08.003
37. Dickerson BC, Salat DH, Greve DN, Chua EF, Rand-Giovannetti E, Rentz DM, *et al.* (2005): Increased hippocampal activation in mild cognitive impairment compared to normal aging and AD. *Neurology* 65. https://doi.org/10.1212/01.wnl.0000171450.97464.49
38. Kwak K, Stanford W, Dayan E (2022): Identifying the regional substrates predictive of Alzheimer's disease progression through a convolutional neural network model and occlusion. *Hum Brain Mapp* 43: 5509–5519.
39. Kwak K, Niethammer M, Giovanello KS, Styner M, Dayan E (2022): Differential Role for Hippocampal Subfields in Alzheimer's Disease Progression Revealed with Deep Learning. *Cerebral Cortex* 32. https://doi.org/10.1093/cercor/bhab223
40. Das SR, Xie L, Wisse LEM, Vergnet N, Ittyerah R, Cui S, *et al.* (2019): In vivo measures of tau burden are associated with atrophy in early Braak stage medial temporal lobe regions in amyloid-negative individuals. *Alzheimer's and Dementia* 15. https://doi.org/10.1016/j.jalz.2019.05.009
41. Timmers T, Ossenkoppele R, Wolters EE, Verfaillie SCJ, Visser D, Golla SSV, *et al.* (2019): Associations between quantitative [18F]flortaucipir tau PET and atrophy across the Alzheimer's disease spectrum. *Alzheimers Res Ther* 11. https://doi.org/10.1186/s13195-019-0510-3
42. Therriault J, Pascoal TA, Lussier FZ, Tissot C, Chamoun M, Bezgin G, *et al.* (2022): Biomarker modeling of Alzheimer's disease using PET-based Braak staging. *Nat Aging* 2: 526–535.
43. Halawa OA, Gatchel JR, Amariglio RE, Rentz DM, Sperling RA, Johnson KA, Marshall GA (2019): Inferior and medial temporal tau and cortical amyloid are associated with daily functional impairment in Alzheimer's disease. *Alzheimers Res Ther* 11. https://doi.org/10.1186/s13195-019-0471-6
44. Woodworth DC, Sheikh-Bahaei N, Scambray KA, Phelan MJ, Perez-Rosendahl M, Corrada MM, *et al.* (2022): Dementia is associated with medial temporal atrophy even after accounting for neuropathologies. *Brain Commun* 4. https://doi.org/10.1093/braincomms/fcac052

45. Morbelli S, Bauckneht M, Arnaldi D, Picco A, Pardini M, Brugnolo A, *et al.* (2017): 18F–FDG PET diagnostic and prognostic patterns do not overlap in Alzheimer's disease (AD) patients at the mild cognitive impairment (MCI) stage. *Eur J Nucl Med Mol Imaging* 44. https://doi.org/10.1007/s00259-017-3790-5
46. Robitaille AL, Webber QMR, Turner JW, Vander Wal E (2021): The problem and promise of scale in multilayer animal social networks. *Curr Zool* 67. https://doi.org/10.1093/cz/zoaa052
47. Hammoud Z, Kramer F (2020): Multilayer networks: aspects, implementations, and application in biomedicine. *Big Data Anal* 5: 1–18.
48. Taylor D, Caceres RS, Mucha PJ (2017): Super-resolution community detection for layer-aggregated multilayer networks. *Phys Rev X* 7: 1–12.
49. Wilson JD, Palowitch J, Bhamidi S, Nobel AB (2017): Community extraction in multilayer networks with heterogeneous community structure. *Journal of Machine Learning Research* 18.
50. Radicchi F, Bianconi G (2017): Redundant interdependencies boost the robustness of multiplex networks. *Phys Rev X* 7. https://doi.org/10.1103/PhysRevX.7.011013
51. Kumar R, Singh A (2020): Robustness in Multilayer Networks under Strategical and Random Attacks. *Procedia Computer Science*, vol. 173 173. https://doi.org/10.1016/j.procs.2020.06.013
52. Liu X, Maiorino E, Halu A, Glass K, Prasad RB, Loscalzo J, *et al.* (2020): Robustness and lethality in multilayer biological molecular networks. *Nat Commun* 11. https://doi.org/10.1038/s41467-020-19841-3
53. Song J, Birn RM, Boly M, Meier TB, Nair VA, Meyerand ME, Prabhakaran V (2014): Age-related reorganizational changes in modularity and functional connectivity of human brain networks. *Brain Connect* 4. https://doi.org/10.1089/brain.2014.0286
54. Contreras JA, Avena-Koenigsberger A, Risacher SL, West JD, Tallman E, McDonald BC, *et al.* (2019): Resting state network modularity along the prodromal late onset Alzheimer's disease continuum. *Neuroimage Clin* 22. https://doi.org/10.1016/j.nicl.2019.101687
55. Sadiq MU, Langella S, Giovanello KS, Mucha PJ, Dayan E (2021): Accrual of functional redundancy along the lifespan and its effects on cognition. *Neuroimage* 229. https://doi.org/10.1016/j.neuroimage.2021.117737
56. Langella S, Mucha PJ, Giovanello KS, Dayan E (2021): The association between hippocampal volume and memory in pathological aging is mediated by functional redundancy. *Neurobiol Aging* 108. https://doi.org/10.1016/j.neurobiolaging.2021.09.002
57. Stanford WC, Mucha PJ, Dayan E (2022): A robust core architecture of functional brain networks supports topological resilience and cognitive performance in middle-and old-aged adults. https://doi.org/10.1073/pnas